Military Technical College
Kobry El-Kobbah
Cairo, Egypt

10th International Conference
On Aerospace Sciences&
Aviation Technology

A Preliminary Design for Multistage Axial Flow Compressors

Part II: Case study

Ahmed F. Abdel Azim*, Ahmed Hamed+ and Wael Shehata+

ABSTRACT

The computer package developed for the preliminary design of multistage axial compressor described in part (I) is applied here for the design of compressor of a typical aeroengine.This compressor is in close proximity to compressor in the CF6-60 turbofan engine. For the same design conditions, the calculated compressor has the same number of stages and layout as that of the CF6 engine. Detailed results concerning both aerodynamic and mechanical designs are presented here.

KEY WORDS

Multistage Axial Compressor, Two Dimensional, hub-to-tip variation, Blade geometry, CF6 turbofan

NOMENCLUTURE

A	annulus area	α	stator angle
C_a	axial velocity	β	rotor angle
C_{DA}	annulus drags coefficient	ψ	stream potential function
C_{DP}	profile drag coefficient	ϕ	velocity potential function
C_{DS}	secondary loss coefficient	η	efficiency
C_D	total drag coefficient	λ	work- done factor
C_u	whirl velocity	Λ	degree of reaction
M	Mach number	σ_{ct}	centrifugal tensile Stress
$\dot{m}$	mass flow rate	ζ	hub-tip ratio

* Professor and head, Mechanical Power Engineering Dept, Zagazig University.
+ Research engineer, Egypt Air co.

N	rotational speed ,number of stages	**Subscripts**	
R	gas constant	1, 2	inlet, outlet
r	radius	t	tip
T_o	total temperature	m	mean

1- INTRODUCTION

Compressor design is a challenging task where team of different specializations including aerodynamistis, mechanical and production engineers as well as metallurgists have to work together. On the basis of their long-accumulated know-how, aeroengine manufacturers develop the modules-including the compressors-for achieving high performance, high durability, high reliability, low noise, low emission, compact and light-weight objectives. Detailed explanations are given by manufacturers of aeroengines like Pratt&Whitney [1], Rolls-Royce [2], Snecma [3], IHI [4],...etc. Preliminary design of the multi-stage compressor represents the first step of the successive detailed design process. Such a procedure is treated in recent publications like Saravananamuttoo [5], and also the most recent publication of the Von Karman Institute for fluid Dynamics [6] where the preliminary design is given by Joachim Kurzke.Kurzke [7] also developed a computer package to calculate the design and off-design performance of gas turbine. Other packages for axial compressor design are available on internet; refer to [8, 9] as examples. In this paper, an application for the computer package described in part (I) of this paper will be employed for the design of a high pressure compressor similar to that found in the turbofan engine CF6.Reasonable agreement between the calculated results and those of the CF6 available in the open literature is noticeable .The CF6 engine was selected as it represents one of the famous power plants in the aviation field. Some important data of CF6 together with similar turbofan engines is listed in table (1).

Table (1) Survey for the characteristic of high pressure compressors in several high bypass ratio turbofan engines.

Engine	CFM 56-7B18	CFM 56-7B26	CFM5 6-5c2	CFM5 6-5c4	CFM5 6-2-C1	RB211-524G/H	RB211 -535	CF6-80C2	CF6-80E1-A2	CF6-80E1-A4
Max takeoff(KN)	82.2	117.4	138.7	151.2	97.8	257.9	178.3	233	292	900
Airflow (Kg/s)	302.5	355.1	465.8	483	788	-	-	808	868	880
Bypass ratio	5.6	5.1	6.6	6.4	6.0	4.1	4.3	5	5.3	5.3
Overall pressure ratio	32.3	32.6	37.4	38.3	31.3	34.5	25.8	-	-	-
Fan Diameter (mm)	1549	1549	1836	1836	1734	2192	1882	2362	2444	2444

2- SOFTWARE

The following softwares are used in the present analysis,
1-MAPLE program is the module used for preliminary design to determine the 2-D and quasi -3D aero-thermodynamic parameters (flow angels, velocities, pressure, temperatures...etc.)and to determine the basic compressor dimensions (radii, blade height).
2- COMPUFOIL program is used for generation of the aerofoil section.
3-MECHANICAL DESKTOP POWER PACK is used to generate 3-D blade shape.

3- CASE STUDY

Based on the survey of the high pressure compressors of turbofan engines, the following data are selected as input to the developed computer package

$T_{o1}=291$ K	$P_{o1}=104000$ pa	$m^{\cdot}=52.21$ kg/s
$N=9800$ rpm	$\Delta T_{os}=28$ K	$\zeta=0.44$
$\gamma=1.4$	R=287 j/Kg.k	$\eta_s=0.9$
η_c=0.9	$C_p=1005$ j/kg.k	$C_a=200$ m/s
$R_c=14$	$\alpha_1=0$	

The package provides the number of stags to be14.Moreover the dimensions of the inlet and outlet sections of the compressor as well as the blade height of stator and rotor blade rows of the 14 stages are calculated .Thus the layout of compressor is shown in figure (1).On the same figure, the layout of the aeroengine CF6-60 where its high pressure compressor (HPC) have the same pressure ratio, is illustrated. Reasonable agreement between both geometries is shown .Moreover; both of the calculated compressor and the HPC of CF6 have the same number of stages. The mean flow characteristics, pressure and temperature variations along the 14 stages are plotted in figure (2).Figure (2a) decomposes the contribution of each stage to the total pressure rise. Figure (2b) illustrates also the temperature build up through the successive stages .The total temperature rise in the compressor is 379.3 K. Velocity triangles for the mean section for first and last stages together with stage 7 as intermediate stage are plotted in figure (3)These velocity triangle have the same rotational speed (U)and axial velocity (C_a).The flow enters the first stage axially ($\alpha_1=0$).then for the 7th stage, α_1 has a finite value which further increase for the last stage .The variation of the angles $\alpha_1, \beta_1, \alpha_2$ and β_2 at the mean section within the different stages is illustrated in figure (4).The efficiency variation for the different stages is plotted in figure (5).The initially assumed stage efficiency was 0.9. This efficiency is calculated for each stage based on its actual flow angles employing cascade data of typical compressor blading[5].These calculations yielded stage efficiency varying from 0.895 to 0.913. Figure (6) shows the variation of centrifugal tensile and gas bending stresses as well as the factor of safety against the stage number for titanium rotor blade. The obtained factor of safety based on the yield strength of titanium alloy varies from 2.5 to 4.8. While figure (7) illustrates the gas bending stress and factor of safety for the stator blade rows manufactured from steel alloy. The state of stress for stator does not include centrifugal tensile stresses. Employing a steel alloy as a typical stator material and based on its yield strength,

the factor of safety ranged from 1.3(last stage)to 5.4 (first stage) The absolute velocity variation (C) within the compressor is shown in figure (8) which as expected has a saw- teeth shape for any stage .The absolute velocity at the rotor inlet C_1 increases to C_2at the rotor outlet .Next it drops again to C_3=C_1 at the inlet of the stator of the succeeding stage and so on for all the compressor stages .Next, the radial variation of the air flow parameters is calculated. Figure (9)represents the variations of the air angles($\alpha_1, \alpha_2, \beta_1, \beta_2$) for stage number (1) using Free vortex blading.Since the flow enters axially at the first stage then $\alpha_1 = 0$ along the blade height, while α_2 drops nearly 20° from hub-to-tip .Both β_1 and β_2 increase from hub to tip .The variation of β_2 is nearly 50° across the blade .The variations in both α_2 and β_2 illustrate the large twist requested for such a type of blading and resembles one of the disadvantages of free vortex design method. Figure (10) represents the variation of air angels for stage (2) using Constant reaction method. Such a design method also showed large variations (around30°)in the stator inlet angle (α_1)and the rotor outlet angle (β_2). Figure (11) represents the variation of air angels for stage (6) using First power method. In such a design method ,the maximum variation in the angles over the blade height is nearly 15°. Figure (12) represents the variation of air angels for stage (7) using Exponential method. Here ,the rotor's outlet has to be twisted some 22° to match the β_2 variation .As shown from this figures ,the first power method yields the minimum blade angle variation for both stator and rotor blades. The variation of the degree of reaction across the blade height is shown in Fig (13) for stage number (1) using free vortex design, figure (14)for stage number(6)using first power design and figure (15) for stage number (14) using exponential design method. Also figures (12)through (14) indicate that the free vortex design has the largest variation of Λ along the blade height (from 0.31-0.86),while the exponential method yields the smallest variation in the degree of reaction .As sited from this results, the free vortex blading is the worst design method due to its large blade twist and large variation in the degree of reaction . The blade shape for the first stage obtained using free vortex method is illustrated in fig (16) for both stator and rotor blade rows. The large rotor blade twist is clarified in such a 3-D illustration . The blade shape for stage (3) obtained using first power method is illustrated in fig (17) for both stator and rotor blade rows. Such an isometric illustration assures that the rotor blade has less twist for the first power method compared to the free vortex method .However ,the stator shape resembles larger twist in this method compared to the free vortex method. The blade shape for stage (4) obtained using exponential method is illustrated in figure (18) for both stator and rotor blade rows. The stator blade twist is very small and represent an advantage for this exponential method. The blade shape for stage 7 and 8 obtained using constant reaction method is illustrated in fig (19) for rotor blade row. The rotor blade twist here is also small. Figure (20) represents the twist for both stator and rotor blade rows. By the symbol $\Delta\alpha_1$ (for example), the difference between α_1 values from hub to tip is meant. Similar variations for other angles $\beta_1, \alpha_2, \beta_2$ are also plotted for all the compressor stages using the four design methods. For sure, the best method is that which yields the minimum variation from hub to tip. For the first power and exponential design methods, variation in the axial velocities are encountered .Figure (21) represents the variation in C_{a1}, C_{a2} for stage number (5) using exponential method. While figure (22) illustrates these variation for stage number (12) using first power method. Both

figures (20,21)outline that C_{a1} and C_{a2} has a maximum value at root and drop to minimum value at tip. The variation in these axial velocities from hub-to-tip is nearly 40 m/s which represent 25% from its value at the mean section .The corresponding velocity triangles for the 6th stage using exponential method is shown in figure (23).The velocity triangle for the 12th stage using first power method across the blade height is shown in figure (24) Moreover the variation of the relative and absolute Mach number in the radial direction is plotted in figure (25)for the first stage and figure (26)for stage number (11)using the constant reaction method.

4- CONCLUSIONS

1- The computer package described in part (I) of this paper is applied here for a case study very close to the HPC of the CF6 turbofan engine.
2- For a pressure ratio of 14 ,14 stage is necessary to achieve such a pressure ratio.
3- The annulus dimensions and blade heights of the fourteen stages are calculated.
4- Layout of the compressor is obtained.
5- To account for the radial variation of the flow angles at the inlet and outlet of both rotors and stators, four different methods are employed;namely,free vortex, exponential ,first power and constant reaction.
6- The results assured the disadvantages of free vortex blading; namely, large rotor blade twist and also large variation in the degree of reaction from hub to tip.
7- The first power method yields smaller twist for the rotor but larger twist for the stator in comparison with the free vortex method
8- The calculated stage efficiency is nearly same as the previously assumed value.
9- The factor of safety based on the stresses on either rotor or stator are calculated for two materials namely titanium and steel alloys.

REFERENCES

1- The Aircraft Gas Turbine Engine and its Operation,P&W Oper.Instr.200,1988
2- The Jet Engine ,Rolls-Royce plc,4th ed.,1986
3- AN,Snecma Sales Brochure,CFM56 Family of Engines,1990
4- Breakthrough Research &Engineering Division, Aero-Engine &Space Operations Brochure,Ishikawajima-Harima Heavy Industries Co.(IHI),2002.
5- Saravananamuttoo ,H. I. H., Rogers , G.F.C. and Cohen , H., Gas Turbine Theory , Prentice – Hall , 5th ed., 2001
6- Aero-Engine Design :A State of the Art ,VKILS 2002-2003,7-11 April 2003
7- WWW. gasturb.de and WWW.conceptseti . com (GasTurb : A program to calculate Design and off-design performance of Gas Turbines, Kurzke , J.,1998)
8- WWW.aircraftenginedesign.com (A program for the Design of Aircraft Engine), Mattingly , J. D. , 1998
9- http://turbo.snu.ac.kr/software/cadac.htm(A computer aided design of axial flow compressor).

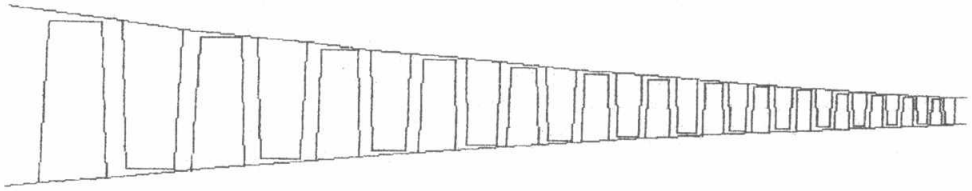

(a) Present calculation

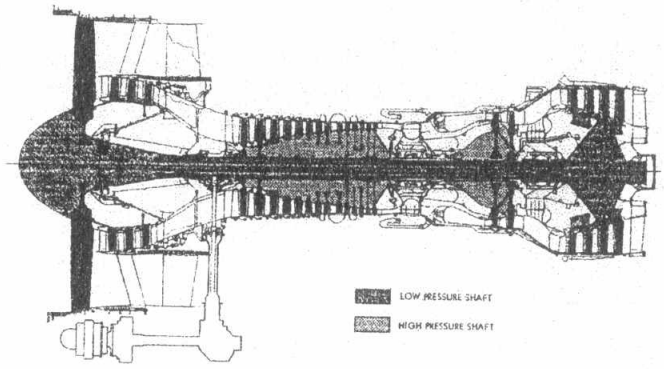

(b) HPC for CF6-60

Fig.1 Layout of the compressor based on the present analysis against its similar HPC in CF6-60 engine

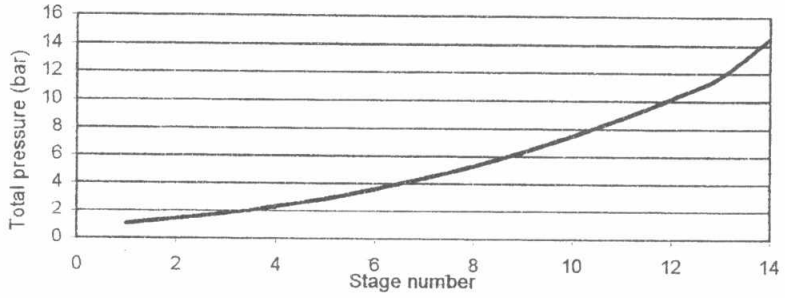

(a)Total pressure variation

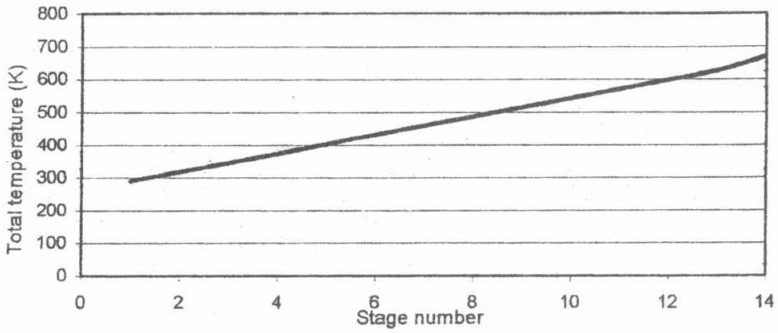

(b)Total temperature variation

Fig.2 Variation of total temperature and pressure within the compressor

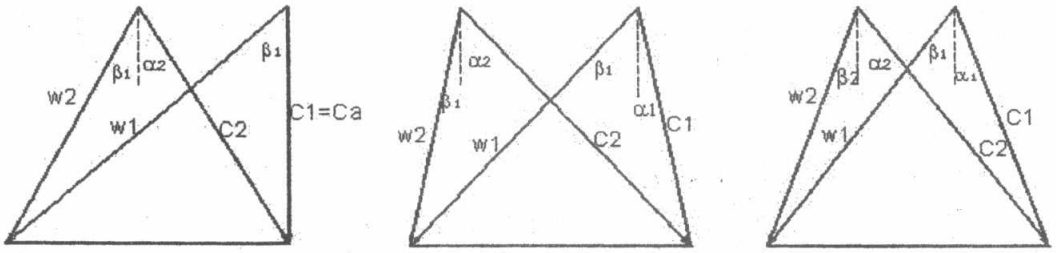

(a)First stage (b) Stage number 7 (c) Last Stage

Figure (3) Velocity triangle at mean diameter

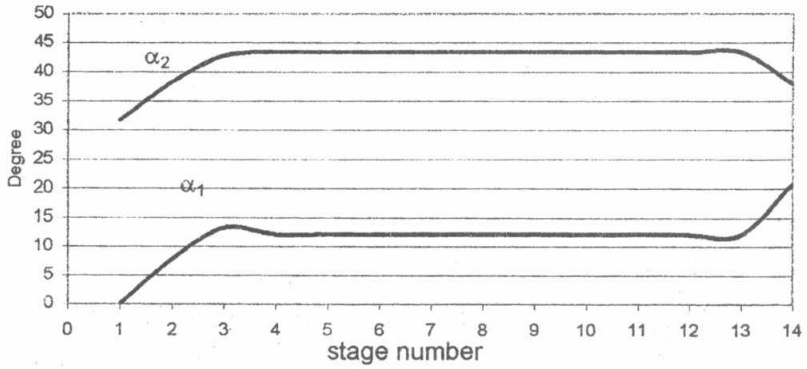

(a) stator angles

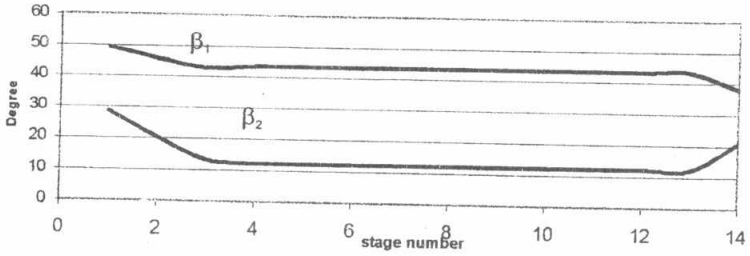

(b) rotor angels

Fig. 4 Variation of the flow angles through different stages

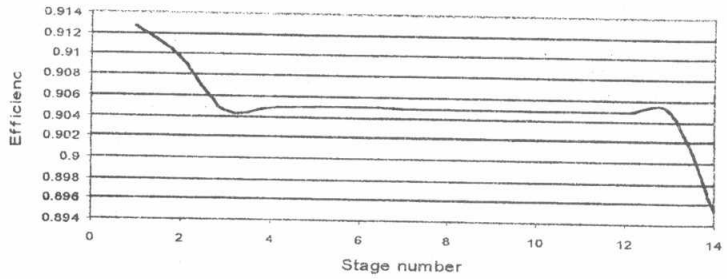

Fig.5 Compressor efficiency versus stage number

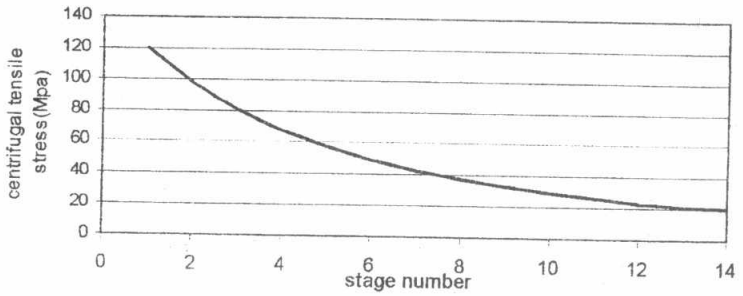

(a) Centrifugal tensile stress

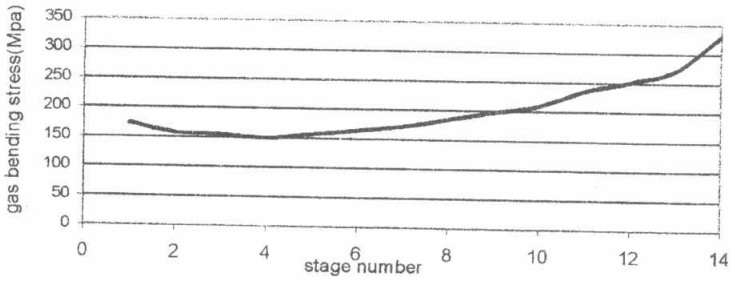

(b) Gas bending stress

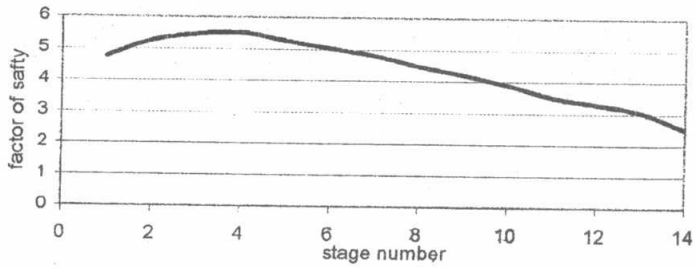

(c) Factor of safety

Fig.6 Variation of stresses and factor of safety versus stage number for titanium rotor blade

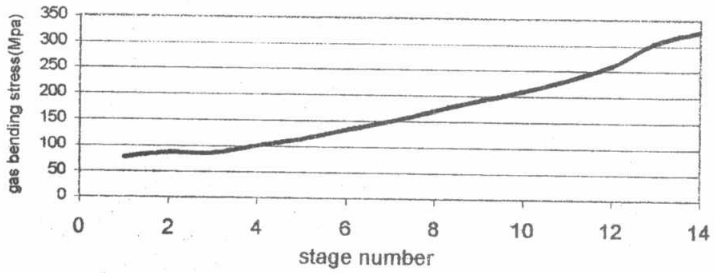

(a)Gas bending stress

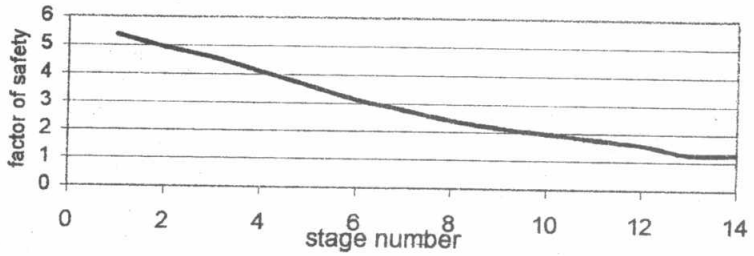

(b)Factor of safety

Fig.7 Gas bending stresses and Factor of safety versus stage number in steel alloy stator blades

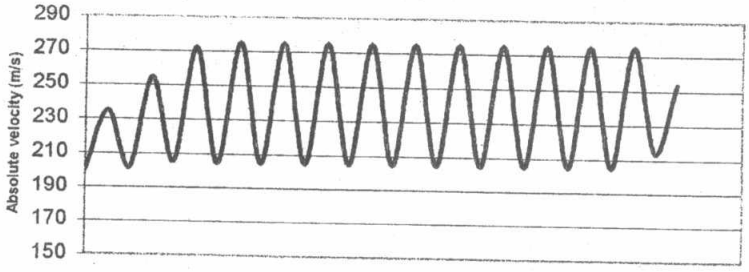

Fig.8 Absolute velocity distribution inside the compressor

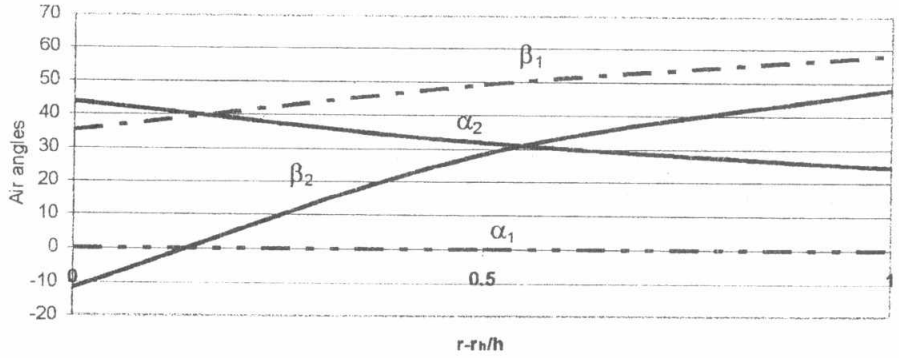

Fig.9 Variation of air angles for stage number 1 using free vortex design

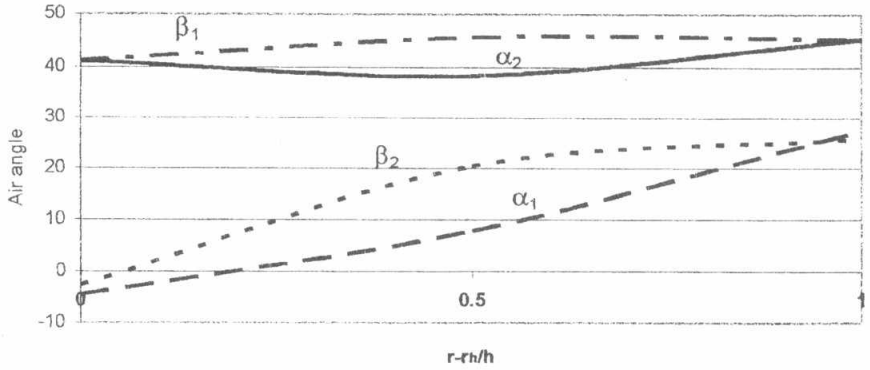

Fig.10 Variation of air angles for stage number 2 using constant reaction design

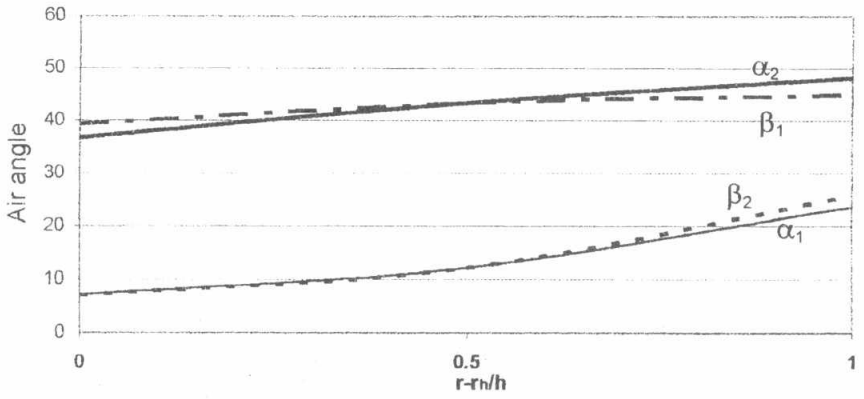

Fig.11 Variation of air angles for stage number 6 using First power design

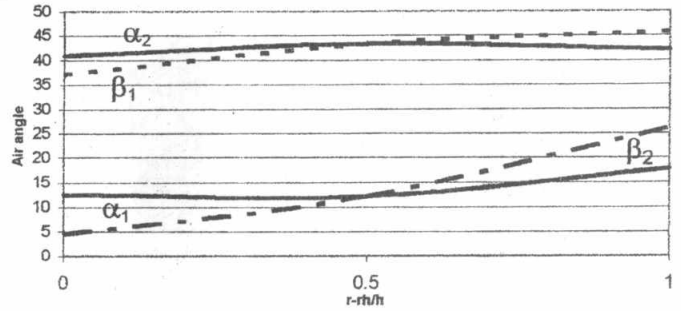

Fig.12 Variation of air angles for stage number 7 using exponential design.

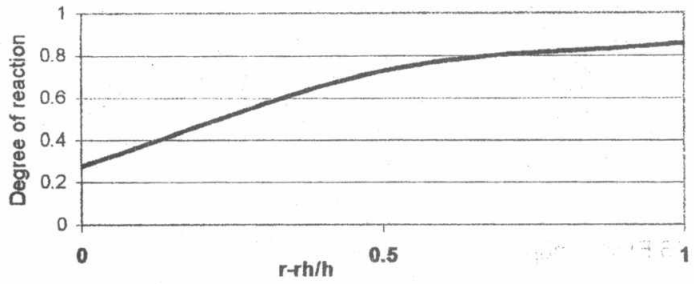

Fig.13 Variation of the degree of reaction from hub to tip for stage number 1 using free vortex design

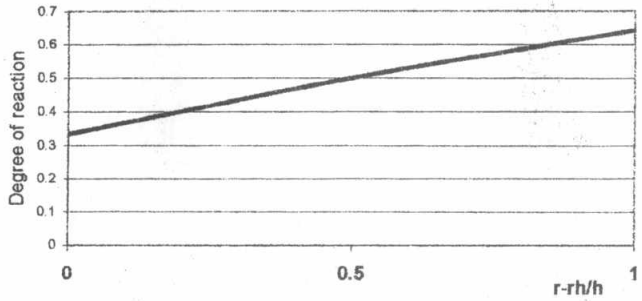

Fig.14 Variation of the degree of reaction from hub to tip for stage number 6 using first power design

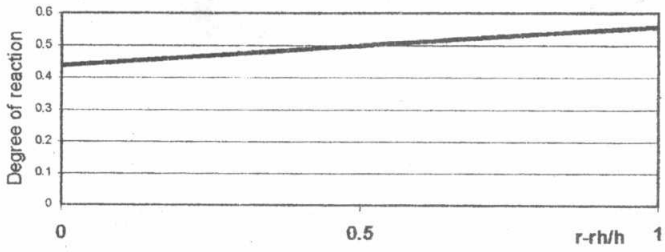

Fig.15 Variation of the degree of reaction from hub to tip for stage number 14 using exponential design

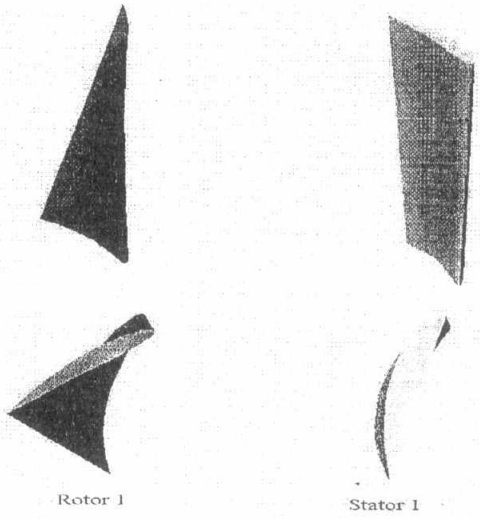

Fig .16 Blade shape of stage number 1 using free vortex method

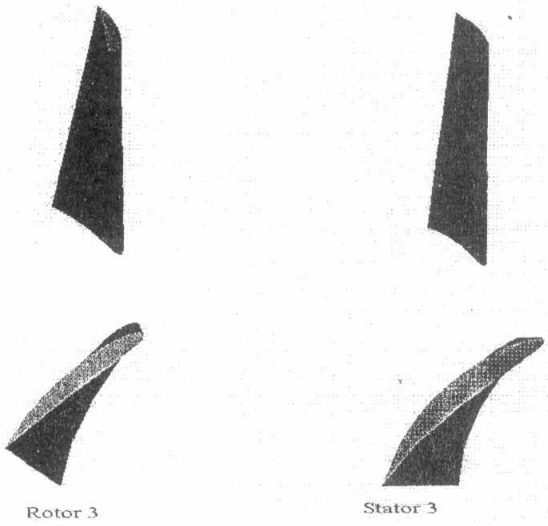

Fig .17 Blade shape of stage number 3 using First power method

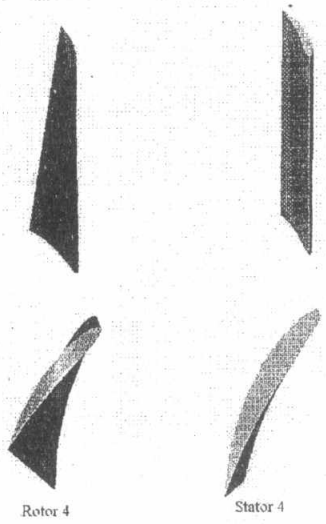

Fig.18 Blade shape of stage number 4 using exponential method

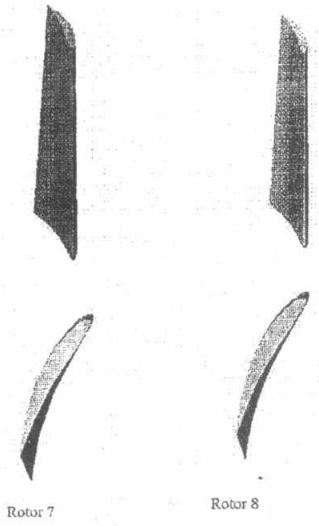

Fig.19 Blade shape of stages number 7,8 using constant reaction method

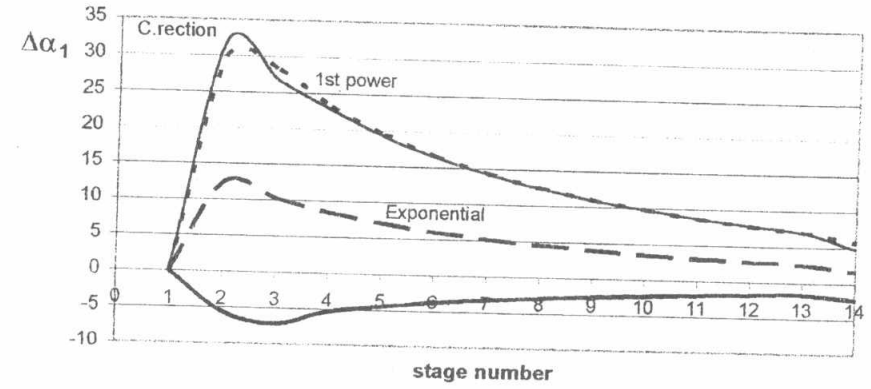

(a) Difference between α_1

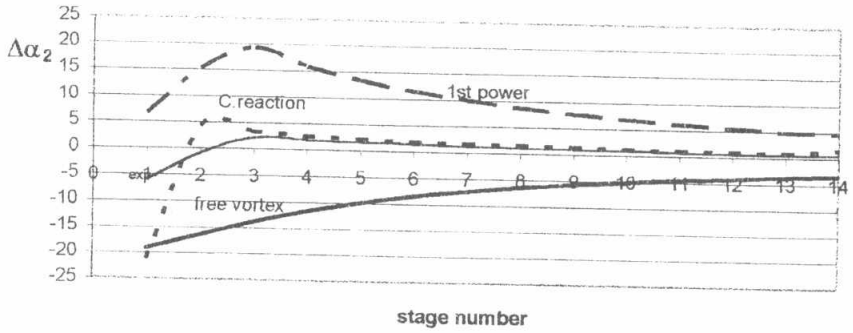

(b) Difference between α_2

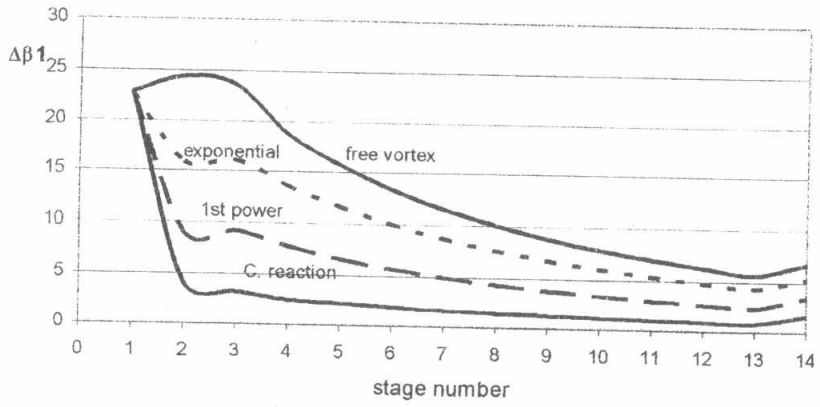

(c) Difference between β_1

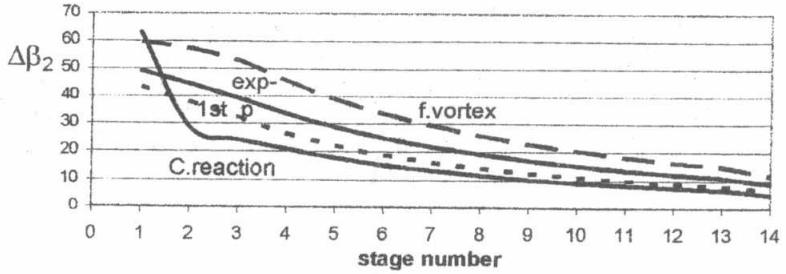

(d)Difference between β_2

Fig.20 Twist for both stator and rotor

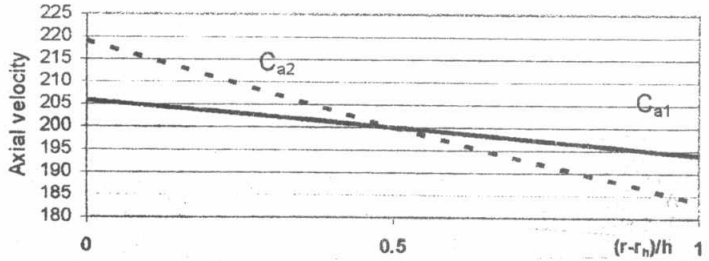

Fig .21 Variation of axial velocity for stage number (5) using exponential method

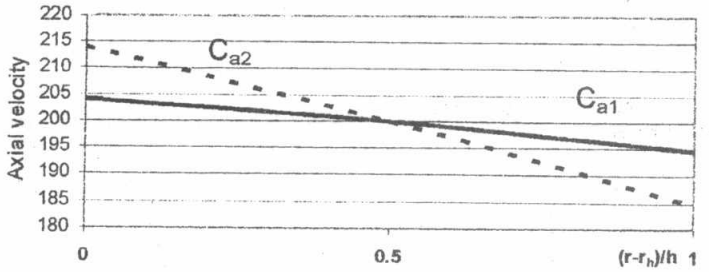

Fig .22 Variation of axial velocity for stage number (12) using first power method

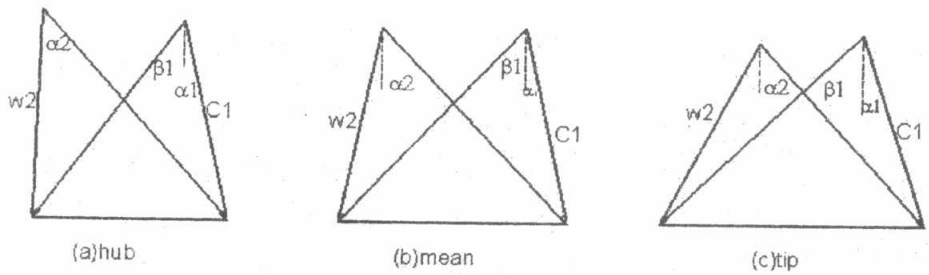

(a)hub (b)mean (c)tip

Fig.23 Velocity triangle using exponential method

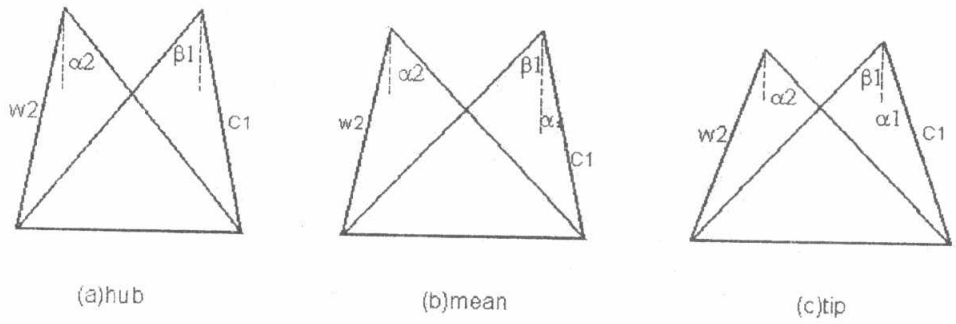

(a)hub (b)mean (c)tip

Fig.24 Velocity triangle using first power method

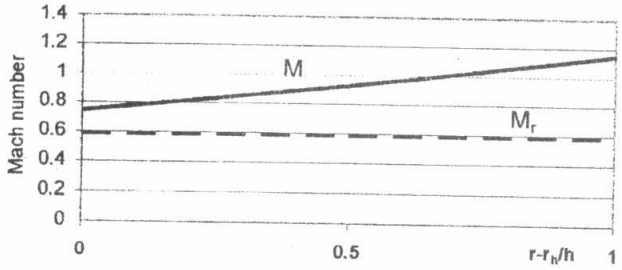

Fig.25 Variation of relative and absolute Mach number for stage number 1 using constant reaction design

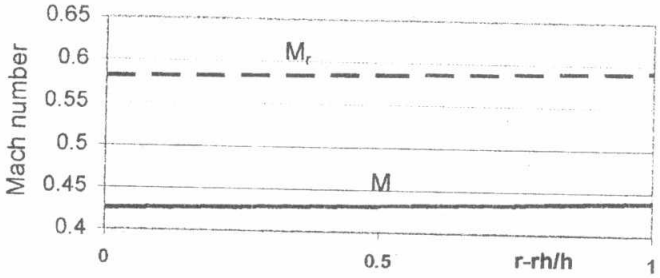

Fig.26 Variation of relative and absolute Mach number for stage number 11 using constant reaction design